Diagn Interv Radiol 2021; 27: 621–632

CHEST IMAGING

REVIEW

Chest CT findings in patients with coronavirus disease 2019 (COVID-19): a comprehensive review

Jinkui Li
Ruifeng Yan
Yanan Zhai
Xiaolong Qi
Junqiang Lei

ABSTRACT

The objective of this review was to summarize the most pertinent CT imaging findings in patients with coronavirus disease 2019 (COVID-19). A literature search retrieved eligible studies in PubMed, EMBASE, Cochrane Library and Web of Science up to June 1, 2020. A comprehensive review of publications of the Chinese Medical Association about COVID-19 was also performed. A total of 84 articles with more than 5340 participants were included and reviewed. Chest CT comprised 92.61% of abnormal CT findings overall. Compared with real-time polymerase chain reaction result, CT findings has a sensitivity of 96.14% but a low specificity of 40.48% in diagnosing COVID-19. Ground glass opacity (GGO), pure (57.31%) or mixed with consolidation (41.51%) were the most common CT features with a majority of bilateral (80.32%) and peripheral (66.21%) lung involvement. The opacity might associate with other imaging features, including air bronchogram (41.07%), vascular enlargement (54.33%), bronchial wall thickening (19.12%), crazy-paving pattern (27.55%), interlobular septal thickening (42.48%), halo sign (25.48%), reverse halo sign (12.29%), bronchiectasis (32.44%), and pulmonary fibrosis (26.22%). Other accompanying signs including pleural effusion, lymphadenopathy and pericardial effusion were rare, but pleural thickening was common. The younger or early stage patients tended to have more GGOs, while extensive/multilobar involvement with consolidation was prevalent in the older or severe population. Children with COVID-19 showed significantly lower incidences of some ancillary findings than those of adults and showed a better performance on CT during follow up. Follow-up CT showed GGO lesions gradually decreased, and the consolidation lesions first increased and then remained relatively stable at 6–13 days, and then absorbed and fibrosis increased after 14 days. Chest CT imaging is an important component in the diagnosis, staging, disease progression and follow-up of patients with COVID-19.

An ongoing outbreak of novel virus pneumonia caused by the severe acute respiratory syndrome coronavirus 2 (SARS-CoV-2) was first reported in Wuhan, Hubei province, China in December 2019 (1, 2), and the causal disease was named as coronavirus disease 2019 (COVID-19) (3). COVID-19 has become a world-wide pandemic due to its rapid transmission. Up to June 29, 2020, the global number of confirmed cases has exceeded 1 019 000. According to Chinese data, the overall mortality rate has been estimated to be about 3.6% (4).

At present, real-time reverse transcription polymerase chain reaction (RT-PCR) has been the clinically acceptable reference standard for definitive diagnosis of COVID-19 infection (5, 6). However, the RT-PCR assay has high specificity but low sensitivity, with overall positive rate being about 30% to 60% at initial presentation (7, 8). These low rates may restrict prompt isolation and diagnosis of infected patients. Besides, RT-PCR could not evaluate and predict the development and prognosis of the disease. Chest computed tomography (CT) has been revealed to have higher sensitivity (60%–98%) than RT-PCR in early detection of COVID-19 with typical appearance of viral lung infection (7, 9, 10) and plays an important role in monitoring the course of pneumonia. A number of cases presented with chest CT abnormality before symptomatic and positive RT-PCR highlight the value of CT in early identification of this disease (7, 11). Having a correct understanding of the typical CT features associated with COVID-19 is important for radiologists.

A growing number of related literature about CT imaging features of COVID-19 has been published. There are a few systematic reviews and meta-analysis of CT evaluating COVID-19

From the Department of Radiology (J.L., R.Y., Y.Z., J.L. ✉ *leijq1990@163.com*), the First Hospital of Lanzhou University, Intelligent Imaging Medical Engineering Research Center, Accurate Image Collaborative Innovation International Science and Technology Cooperation, Lanzhou, China; The first Hospital of Lanzhou University (X.Q.), Lanzhou, Gansu, China.

Received 12 May 2020; revision requested 16 June 2020; last revision received 23 July 2020; accepted 26 August 2020.

Published online 23 October 2020.

DOI 10.5152/dir.2020.20212

You may cite this article as: Li J, Yan R, Zhai Y, Qi X, Lei J. Chest CT findings in patients with coronavirus disease 2019 (COVID-19): a comprehensive review. Diagn Interv Radiol 2021; 27: 621–632

with a latest searched time of Apr 12, 2020 (12–16); however, it has been a while since the outbreak of COVID-19 and the relevant articles have been constantly updated. Besides, almost all the study subjects were from China. Updates of review of COVID-19 are necessary when new evidence emerges. This is a global public health problem, so we need to know more about COVID-19 pneumonia: the characteristics on CT, and the correlation of CT findings with clinical severity and progression, change during the time course. Therefore, the aim of this review was to review the published literature and summarize the most pertinent CT imaging findings as well as follow-up changes of COVID-19 and to provide evidence-based guidance for clinical practice.

Methods

Literature search

The literature search was conducted for retrieving eligible studies indexed in PubMed, EMBASE, Cochrane Library and Web of Science, as well as SinoMed, China National Knowledge Infrastructure (CNKI) and Wanfang online databases as of June 1, 2020. We applied the following search terms to titles and abstracts in database: "2019 novel coronavirus pneumonia", "coronavirus disease 2019 virus", "COVID-19", "2019-nCoV", "SARS-CoV-2" and "CT", "Computed tomography", "Computed X Ray Tomography", "Tomography, X-Ray Computed" for English studies. In addition, similar search strategy (in Chinese) was carried out for relevant Chinese articles of the Chinese Medical Association. Reference lists from selected studies were manually searched for additional potentially eligible articles.

Main points

- The typical initial CT findings in COVID-19 patients were peripheral ground-glass opacity (GGO), mixed GGO with consolidation, or consolidation.
- The younger or early stage patients tended to have more GGOs, while extensive/multilobar involvement with consolidations was prevalent in the older or severe population.
- Follow-up CT showed GGO lesions gradually decreased, and the consolidation lesions first increased and then remained relatively stable at 6–13 days, and then absorbed and fibrosis increased after 14 days.
- Chest CT imaging is an important component of the diagnostic work-up and management in patients with COVID-19.

Study eligibility and selection

All relevant studies were identified by two reviewers (J.Li and R.Y.). Patients with clinical suspicion of pneumonia based on symptoms or clinical diagnosis and with CT examination were evaluated. The following criteria were applied to select the studies: 1) a dedicated research article; 2) a confirmed diagnosis of COVID-19 pneumonia based on RT-PCR or genetic sequence assay; 3) a detailed description of radiological patterns on CT images or data of imaging changes on follow-up CT. Case reports and studies of less than 10 cases were eliminated from the analysis. Additionally, review articles and studies with insufficient subject identification were excluded. In the case of redundant reporting of patient populations, only the study with the largest population was included. We only considered original studies published in English and Chinese.

Two readers (J.Li and R.Y.) independently browsed titles and abstracts of all search results, and selected eligibility for further full texts. Then the full texts were reviewed in detail, and those meeting the defined criteria were enrolled in the final review. Any discrepancy was resolved by consensus with senior authors (J.Lei).

Data extraction and analysis

After full text reading, the following data were extracted by one investigator (J.Li) in a standardized spreadsheet: the first author; year of publication; country; study design; sample size; gender proportion; age (year); underlying disease; clinical staging; reconstruction thickness of CT; radiological patterns denoted by CT, which were defined as lung and lobes involved, the distribution (bilateral lung, peripheral, central), morphology, density of lesion (GGO, consolidation, mixed GGO consolidation), pleural effusion, lymphadenopathy, other abnormalities (e.g., interlobular septal thickening, air bronchogram); and imaging changes on follow-up CT (including improvement, progression, no change). Descriptive analysis was used to present pooled demographic information and other data, where applicable.

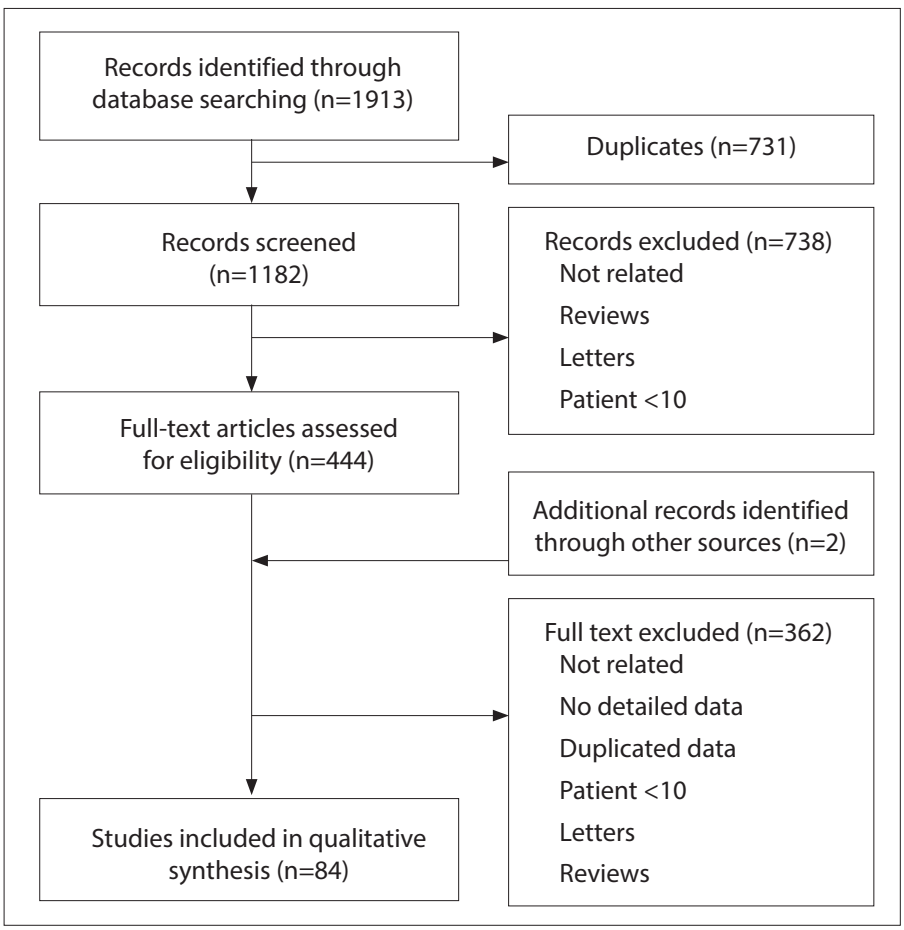

Figure. The process of study screening.

Table 1. Demographic characteristics of the included studies with initial abnormal CT

Author [Ref]	Study design	Country	Sample (n) (male/female)	Age (y) mean±SD (range)	Initial CT(+/-)	Reference standard	Comorbidity
Huang L[17]	R	China	103 (60/43)	57±24 (20-89)	103/0	RT-PCR	/
Lu X[18]	R	China	141 (77/64)	Median 49 (9-87)	141/0	RT-PCR	44
Liu H[19]	R	China	106 (64/42)	57±15 (22-82)	106/0	RT-PCR	9
Bernheim A[10]	R	China	121 (61/60)	45.3 (18-80)	94/27	RT-PCR	/
Song F[20]	R	China	51 (25/16)	49±16 (16-76)	51/0	RT-PCR	11
Pan Y[21]	R	China	63 (33/30)	44.9±15.2 (25–63)	63/0	RT-PCR	/
Liu RR[22]	R	China	33 (20/13)	50±12 (20-70)	30/3	RT-PCR	6
Wu J[23]	R	China	130 (78/52)	43±15 (25-80)	130/0	RT-PCR	/
Long C[24]	R	China	36 (20/16)	44.8±18.2	35/1	RT-PCR	/
Zhou Z[25]	R	China	62 (34/28)	47.25 (20-91)	62/0	RT-PCR	/
Chen Z[26]	R	China	98 (52/46)	43.0±17.2 (4-88)	91/7	RT-PCR	/
Zhou SC[27]	R	China	62 (39/23)	52.8±12.2 (30-77)	62/0	RT-PCR	10
Zhu T[28]	R	China	72 (42/30)	55.6±12.8 (20-83)	72/0	RT-PCR	/
Fan N[29]	R	China	150 (68/82)	Median 56 (17-90)	150/0	RT-PCR	69
Guan C[30]	R	China	53 (25/28)	42 (1-86)	47/6	RT-PCR or genetic sequence assay	/
Han R[31]	R	China	108 (38/70)	45 (21-90)	108/0	RT-PCR	/
Jie B[32]	R	China	24 (16/8)	48.80±17.41 (18-83)	24/0	RT-PCR	7
Li KH[33]	R	China	83 (44/39)	45.5	83/7	RT-PCR	15
Li KW[34]	R	China	78 (38/40)	44.6±17.9	56/22	RT-PCR or genetic sequence assay	33
Li XM[35]	R	China	131 (63/68)	47±15 (20-90)	125/6	RT-PCR	/
Li Y[36]	R	China	53 (29/24)	58±17 (26-83)	49/0	RT-PCR	/
Liu KC[37]	R	China	73 (41/32)	41.6±14.5 (5-86)	67/5	RT-PCR	/
Liu Z[38]	R	China	72 (39/33)	46.2±15.9	69/3	RT-PCR	17
Luo Z[39]	R	China	195 (94/101)	46 (33-59)	170/25	RT-PCR	/
Meng H[40]	R	China	58 (26/32)	42.60±16.56	58/0	RT-PCR	20
Shi H[41]	R	China	81 (42/39)	49.5±11.0	81/0	RT-PCR	59
Wang J[42]	R	China	93 (57/36)	52.1±18.07 (7-89)	93/3	RT-PCR	/
Wang K[43]	R	China	114 (56/58)	Median 53 (23-78)	111/3	RT-PCR	60
Wang M[44]	R	China	66 (43/23)	44±14 (18-75)	66/0	RT-PCR	12
Wu J[45]	R	China	80 (42/38)	44±11 (15-79)	76/14	RT-PCR or genetic sequence assay	15
Yang W[46]	R	China	149 (81/68)	45.11±13.35	132/17	RT-PCR	52
Zhang S[47]	R	China	17 (9/8)	Median 48.6 (23-74)	17/0	RT-PCR	7
Xu Xi[48]	R	China	90 (39/51)	Median 48.6 (18-86)	69/21	RT-PCR	45
Wang X[49]	R	China	40 (26/14)	41.9±12 (21-71)	40/0	RT-PCR	/
Caruso D[50]	P	Italy	158 (83/75)	57±17 (18-89)	60/2	RT-PCR	/
Xu YH[51]	R	China	50 (29/21)	43.9±16.8 (3-85)	41/9	RT-PCR	/
Xiong Y[52]	R	China	42 (25/17)	49.5±14.1 (26-75)	42/0	RT-PCR	13
Bai HX[53]	R	China	219 (119/100)	44.8±14.5 (4-76)	219/37	RT-PCR	71
Yu C[54]	R	China	91 (39/52)	Median 50 (33-62)	67/24	RT-PCR	42
Yang T[55]	R	China	10 (5/5)	24-65	10/0	RT-PCR or genetic sequence assay	1
Hu R[56]	R	China	105 (55/50)	44.38±15.69 (2 m to 88 y)	99/6	RT-PCR	/

Table 1. Demographic characteristics of the included studies with initial abnormal CT (cont'd)

Author [Ref]	Study design	Country	Sample (n) (male/female)	Age (y) mean±SD (range)	Initial CT(+/-)	Reference standard	Comorbidity
Dai H[57]	R	China	234 (136/98)	44.6±14.8 (7-82)	219/15	RT-PCR	/
Zhao W[58]	R	China	118 (60/58)	44.06±13.62 (2-75)	110/8	RT-PCR or genetic sequence assay	37
Yu M[59]	R	China	32 (22/10)	44.44	32/0	RT-PCR	9
Haseli S[60]	R	Iran	63 (38/25)	54.2±14.9 (26-81)	63/0	RT-PCR	/
Hu Q[61]	R	China	46 (27/19)	39.2±9.6 (23-60)	46/0	RT-PCR	/
Liu M[62]	R	China	122 (61/61)	48±15 (15-80)	112/10	RT-PCR	35
Li X[63]	R	China	154 (76/78)	59 (22-88)	154/0	RT-PCR	/
Xiong Z[64]	R	China	421 (214/207)	Median 52	397/24	RT-PCR	195
Liu J[65]	R	China	24 (14/10)	57.9±15.3 (25-75)	24/0	RT-PCR or genetic sequence assay	11
Xie S[66]	R	China	12 (6/6)	40 (30-61)	12/0	RT-PCR	4
Fu F[67]	R	China	55 (33/22)	45 (20-67)	55/0	RT-PCR	/
Wang H[68]	R	China	13 (7/6)	49.5±17.4 (20-72)	13/0	RT-PCR	/
Yin Z[69]	R	China	30 (19/11)	52.7±15.1	30/0	RT-PCR	15
Nie W[70]	R	China	163 (84/79)	40.2±16.3 (9-78)	156/7	RT-PCR	/
Zhang L[71]	R	China	34 (19/15)	Median 49.21 (7-88)	33/1	RT-PCR	13
Ma J[72]	R	China	22 (12/10)	Median 4 y (2 m to 14 y)	19/3	RT-PCR	0
Chen J[73]	R	China	20 (7/13)	7.8±5.4 y (8 m to 14 y)	13/7	RT-PCR or genetic sequence assay	0
Song W[74]	R	China	16 (10/6)	Median 8.5 y (11.5 m to 14 y)	11/5	RT-PCR	0
Xia W[75]	R	China	20 (13/7)	2 y±1.5 m (1 d to 14 y)	16/4	RT-PCR	3
FENG K[76]	R	China	15 (5/10)	7 (4-14)	9/6	RT-PCR	0
Zheng F[77]	R	China	25 (14/11)	Median 4 y (3 m to 14 y)	17/8	RT-PCR	2
Li YJ[78]	R	China	15 (6/9)	8 (4-17)	7/8	RT-PCR	0
Li B[79]	R	China	22 (12/10)	8±6	20/2	RT-PCR	0
Steinberger S[80]	R	China	30 (15/15)	Median 10 y (10 m to 18 y)	7/23	RT-PCR	0
Wu HP[81]	R	China	23 (9/14)	5 y ± 7 m (3 m to 17 y)	12/10	RT-PCR	0
Ma H[82]	R	China	50 (28/22)	2.5 (0.9–7.0)	43/7	RT-PCR	7
Total			5340 (2823/2507)		4809/396		949

R, retrospective; P, prospective; d, days; m, months; y, years; PT-PCR, real-time polymerase chain reaction.

Results

After screening 1913 abstracts, 1182 articles met the inclusion criteria for further full text. Then 84 studies were selected for inclusion in this systematic review after gradually eliminating (10, 17–99). The selection process of the studies is described as a flowchart in Fig.

Abstracted data of including studies with initial CT findings are summarized in Table 1. Of the 67 selected articles (10, 17–82), 51 were in English (10, 20, 21, 24–48, 50–53, 57–69, 71, 74, 75, 77, 79, 80, 82) and 16 were in Chinese (17–19, 22, 23, 49, 54–56, 70, 72, 73, 76, 78, 81). All but one of these studies were retrospective (50). One study was from Italy (50) and one from Iran (60), and all the other study subjects were exclusively from China. There were a total of 5340 participants, with age ranging from 1 day to 91 years. In the adults cohort, males (52.87%, 2823/5340) were slightly more frequent than females. Sample sizes in the studies ranged from 10 to 421 patients. Overall, 33.10% (949/2868) of patients had comorbidities, including diabetes and hypertension commonly seen in adult patients. Of the children with COVID-19, only a few had underlying disease.

The main initial CT findings of the included studies are listed in Tables 2 and 3. CT imaging findings were assessed according to the presence and distribution of parenchymal abnormalities. The abnormal CT findings were present in 92.61% (4961/5357) of the included patients. CT imaging had a lower sensitivity to detect pulmonary abnormality in children (67.70%, 174/257) compared to adult patients (81.02%, 367/453). A total of 48 studies recorded the laterality involvement and 39 studies described the axial distribution, with a majority of bilateral lung involvement (80.32%) and peripheral lung predilection (66.21%). The incidence of right lung involvement (62.72%) was higher than the left (37.28%)

Table 2. Distribution of findings in COVID-19 patients with abnormal CT

Distribution	Number of studies where the corresponding data has been provided for all the patterns	Pooled incidence (according to abnormal CT)
Laterality		
Bilateral	48 [10,17-20,22,23,26,27,29,30,33-35,37-41,43,44,47-51,53-55,57-60,62-67,71,72,74,75,77-81]	2977/3703 (80.39%)
Unilateral	48 [10,17-20,22,23,26,27,29,30,33-35,37-41,43,44,47-51,53-55,57-60,62-67,71,72,74,75,77-81]	726/3703 (19.61%)
Left lung	12[10,17,19,23,29,30,35,40,63,67,72,81]	85/228 (37.28%)
Right lung	12[10,17,19,23,29,30,35,40,63,67,72,81]	143/228 (62.72%)
Axial distribution		
Peripheral	39[17,19,20,22,24,25,27-31,34-36,39-44,59,51-53.55,58,59,63,65-68,70,73,75,79,80,82]	1842/2782 (66.21%)
Central	39[17,19,20,22,24,25,27-31,34-36,39-44,59,51-53.55,58,59,63,65-68,70,73,75,79,80,82]	117/2782 (4.21%)
Central+peripheral	39[17,19,20,22,24,25,27-31,34-36,39-44,59,51-53.55,58,59,63,65-68,70,73,75,79,80,82]	823/2782 (29.58%)
Lobar distribution		
Right upper lobe	21[10,22,24,29,30,33,34,40,41,44,48-51,56,60-62,64,79,80]	1334/7747 (17.22%)
Right medial lobe	21[10,22,24,29,30,33,34,40,41,44,48-51,56,60-62,64,79,80]	985/7747 (12.71%)
Right lower lobe	21[10,22,24,29,30,33,34,40,41,44,48-51,56,60-62,64,79,80]	2087/7747 (26.94%)
Left upper lobe	21[10,22,24,29,30,33,34,40,41,44,48-51,56,60-62,64,79,80]	1484/7747 (19.16%)
Left lower lobe	21[10,22,24,29,30,33,34,40,41,44,48-51,56,60-62,64,79,80]	1857/7747 (23.97%)
Number of lobes affected		
One lobe	19[10,20,21,28,34,35,38-40,44,48,50-52,62,64,67,71,80]	292/1562 (18.69%)
Two lobes	19[10,20,21,28,34,35,38-40,44,48,50-52,62,64,67,71,80]	238/1562 (15.24%)
Three lobes	19[10,20,21,28,34,35,38-40,44,48,50-52,62,64,67,71,80]	220/1562 (14.08%)
Four lobes	19[10,20,21,28,34,35,38-40,44,48,50-52,62,64,67,71,80]	279/1562 (17.86%)
Five lobes	19[10,20,21,28,34,35,38-40,44,48,50-52,62,64,67,71,80]	533/1562 (34.12%)

in cases of unilateral lung involvement. Changes were more prevalent in lower lung zones than the upper or middle lobes.

Pure GGO (57.31%) reported in 88.06% (59/67) of the studies, pure consolidation (24.48%) reported in 85.07% (57/67) of the studies, and mixed GGO with consolidation opacity (41.51%) were all common imaging patterns on CT. The opacity may be associated with other imaging features, such as air bronchogram (41.07%), vascular enlargement (54.33%), bronchial wall thickening (19.12%), crazy-paving pattern (27.55%), reticulation, interlobular septal thickening (42.48%), halo sign (25.48%), reverse halo sign (12.29%), bronchiectasis (32.44%), and pulmonary fibrosis (26.22%). Only a few studies had reported nodules and intralobular septal thickening. Other accompanying signs including pleural effusion, lymphadenopathy and pericardial effusion were rare, but pleural thickening was common.

Although Chen et al. (26) reported the presence of abnormalities per-lesion rather than by per-patient, their results were parallel with the above summary. Of the 701 lesions detected on CT imaging of 91 patients, 80.7% located in the peripheral field. GGO with a crazy paving pattern or interlobular septa thickening were the most common findings (48.8%). Similarly, some lesions presented with air bronchogram (26).

The imaging findings of initial CT scan at different ages were noted in only 3 studies. Young patients and older adults with COVID-19 may share certain CT features (20, 26, 28), but older patients (>60 years) were likely to have more lung involvement, and subpleural line, pleural thickening and consolidation (20, 28). Patients aged ≥45 years had more bilateral lung, lung lobe, and lung field involvement than patients <18 years, and GGO accompanied signs of interlobular septa thickening or a crazy-paving pattern, consolidation, and air bronchogram sign were more common in patients aged ≥45 years, than in those aged ≤44 years (26). Younger patients tended to have more GGOs (20).

We also summarized the imaging features of children and adults with COVID-19 (Table 3). For the child cohort, the presence and distribution of CT imaging findings are similar to those of adult patients. GGO (38.13%) was the most common finding and halo sign (19.77%) was a common ancillary finding in children. Nonetheless, children with COVID-19 showed significantly lower incidences of some ancillary findings than those of adults. Intralobular septal thickening, pulmonary fibrosis and bronchiectasis were not seen in children with COVID-19. There was only one child patient with enlarged lymph nodes (74) and two with pleural effusion (73, 82). No pleural thickening or pericardial effusion had been seen in children yet.

COVID-19 can be divided into mild, moderate, severe and critical types according to its severity (6). A total of 19 studies had mentioned the clinical staging (Table 4). The most frequent clinical staging was moderate (76.63%). Mild type was relatively less common than moderate among children (37.42%). The imaging manifestations of patients with different clinical types of COVID-19 have characteristic manifestations that can overlap. The patients with mild or moderate stage are more likely to present with pure GGO and halo sign (42), while some patients can present with neg-

Table 3. Pooled incidence of various radiological findings on chest CT in COVID-19 patients

	Number of studies where the corresponding data has been provided			Pooled incidence (as per total number of CT performed)		
	All the included patients	Adults alone	Children alone	All the included patients	Adults alone	Children alone
Major patterns of attenuation						
GGO	59[10,17-25,28-41,43-45,47-51,53-56,58-76,78-80]	28[10,17,19,21-23,25,27,28,31,32,35,36,39,43,44,47-50,54,60,61,63,65-68]	8[72-76,78-80]	2650/4624 (57.31%)	1029/2204 (46.69%)	61/160 (38.13%)
Consolidation	57[10,17-25,28-41,43-45,47-54,56,58-60,62-76,79, 80]	26[10,17,21-23,25,27,28,31,32,35,36,39,43,44,48-50,52, 54,60,63,65-68]	7[72-76,79,80]	1135/4637 (24.48%)	376/2140 (17.57%)	23/145 (15.86%)
GGO+consolidation (mixed)	29[10,17,19,20,22-25,28-32,35,36,38,41,43,47,49, 51,56, 58-63,65-68,70,72,73,78-80]	19[10,17,22,23,25,28,31,32,35,36,43,47,49,61,63,65- 68]	5[72,7378-80]	1196/2881 (41.51%)	640/1264 (50.63%)	17/109 (15.60%)
Ancillary findings						
Interlobular septal thickening	30[20,22,29,33-36,41,42,44,45,48-54,56, 57,59-62,65-68,70,72]	15[22,35,44,48-50,52,54,60,61,65-68]	1[72]	1057/2500 (42.28%)	227/914 (24.84%)	1/22 (4.54%)
Intralobular septal thickening	3[37,61,68]	2[61,68]	0	26/132 (19.70%)	15/59 (25.42%)	0
Crazy paving	36[10,19,20,23,25,27-31,33,35-38,40-42,44-46,48- 50,53,59,62,66,67,69-72,75,79,80]	16[10,19,23,25,27,28,31,35,36,38,44,48-50,66,67]	3[72,79,80]	833/3024 (27.55%)	390/1449 (26.92%)	6/76 (7.89%)
Vascular enlargement	18[23,27-29,31,32,35,36,40,42,53,54, 56,66,67,69,71,72,82]	9[23,28,31,32,35,36,54,66,67]	2[72,82]	816/1502 (54.33%)	496/736 (67.39%)	12/72 (16.67%)
Halo sign	16[23,25,31,36,39,40,42,44,50,53,62, 66,72,74,75,80]	7[23,25,31,36,39,44,66]	4[72,74,75,80]	347/1362 (25.48%)	202/624 (32.37%)	17/88 (19.32%)
Reversed halo sign	7[23,36,39,42,53,60,80]	4[23,36,39,60]	1[80]	96/781 (12.29%)	70/439 (15.95%)	1/30 (3.33%)
Air bronchogram	43[18,20,23,25,27-32,34-41,44,46-54,56,57,59,61-63,65-72,74]	24[23,25,27,28,31,32,35,36,38,39,44,47-50,52,54,61, 63, 65-68]	2[72,74]	1439/3504 (41.07%)	683/1643 (41.57%)	3/38 (7.89%)
Bronchial wall thickening	13[10,18,25,33,45,50,53,57,58,62,68,69,77]	4[10,25,50,68]	1[78]	267/1396 (19.12%)	15/354 (4.24%)	2/15 (13.33%)
Bronchiectasis	11[10,27,41,42,44,46,57-60,66,69]	5[10,27,44,60,66]	0	318/980 (32.44%)	24/324 (7.41%)	0
Nodule	4[18,57,60,66]	1[60]	0	150/438 (34.25%)	0/63	0
Cavitation	11[23,35,42,48,50,60-62,66,71,80]	7[23,35,48,50,60,61,66]	1[80]	8/909 (0.88%)	1/630 (0.16%)	0/30 (0)
Pulmonary fibrosis	10[21,27,31,34-36,44,49,52,56]	8[21,27,31,35,36,44,49,52]	0	220/839 (26.22%)	136/563 (24.16%)	0
Accompanying signs						
Pleural effusion	55[10,17-25,27-39,41-45,47,48,50-57,59-63,66-69, 71-73,75,76,78,80,82]	27[10,17,19,21-23,25,27,28,31,32,35,36, 39,43,44,47,48, 50,52,54,55,60,61,63,67,68]	7[72,73,75,76, 78,80,82]	182/4181 (4.35%)	75/2183 (3.44%)	2/172 (1.16%)
Pleural thickening	16[19,22,27,28,31,35,41,42,48,49,53, 54,57,65,66,69]	11[19,22,27,28,31,35,48,49,54,65,66]	0	515/1426 (36.12%)	239/769 (31.08)%)	0
Lymphadenopathy	51[10,17-25,27-39,41-48,50-55,57,59,61-63,66,67,72,74-76,78,80,82]	25[10,17,19,21-23,25,27,28,31,32,35,36,39,43,44,47, 48,51,52,54,55,61,63,67]	7[72,74-76,78,80,82]	237/4081 (5.81%)	162/1999 (8.10%)	1/168 (0.60%)
Pericardial effusion	7[19,20,33,48,50,62,69]	3[19,48,60]	0	17/561 (3.03%)	5/354 (1.41%)	0

ative imaging findings (6, 96). The severe and critical COVID-19 patients usually involve both lungs and multiple lobes, present with consolidation with crazy-paving sign, interlobular septal thickening, pleural thickening, architectural distortion, and bronchiectasis dominantly (33, 42, 47, 51). Besides, intrathoracic lymph node enlargement, pleural effusions and pericardial effusion are more likely to be found in the severe-critical group (33, 42, 47). Li et al. (34) reported that the moderate type had a lower incidence of right upper lobe and middle lobe involvement than severe-critical type.

There were 9 studies evaluating the performance of chest CT in diagnosing COVID-19 (Table 5). CT findings were generally concordant with RT-PCR results, with a sensitivity of 96.14% (1371/1426). However, CT had a low specificity of 40.48% (340/840) in diagnosing COVID-19, similar to the results of a meta-analysis (16). Another study showed that if chest CT was taken as a reference of diagnosis standard for COVID-19, the sensitivity of RT-PCR was 65% (100).

Dynamic changes on chest CT in patients with COVID-19 from disease on-

Table 4. Pooled incidence of clinical types on chest CT in COVID-19 patients

	Number of studies			Pooled incidence (as per total number of CT performed)		
	All the included patients	Adults alone	Children alone	All the included patients	Adults alone	Children alone
Mild	19[17,22,32,34,37,38,51,53,72-74,76-78,81-84]	4[17,22,32,84]	8[72-74,76-78,81,82]	138/1134 (12.17%)	20/262 (7.63%)	58/155 (37.42%)
Moderate	19[17,22,32,34,37,38,51,53,72-74,76-78,81-84]	4[17,22,32,84]	8[72-74,76-78,81,82]	869/1134 (76.63%)	162/262 (61.83%)	92/155 (59.35%)
Severe	19[17,22,32,34,37,38,51,53,72-74,76-78,81-84]	4[17,22,32,84]	8[72-74,76-78,81,82]	82/1134 (7.23%)	64/262 (24.43%)	0 (0)
Critical	19[17,22,32,34,37,38,51,53,72-74,76-78,81-84]	4[17,22,32,84]	8[72-74,76-78,81,82]	45/1134 (3.97%)	16/262 (6.11%)	5/155 (3.23%)

Table 5. Comparing chest CT result with RT-PCR

Author	TP	FP	FN	TN
Deng ZQ[85]	423	71	10	83
Ai T[7]	580	308	20	105
He JL[86]	26	2	8	46
Xie X[11]	155	5	7	0
Caruso D[50]	60	42	2	54
Wen Z[87]	82	7	6	8
Himoto Y[88]	6	4	0	11
Zhu W[89]	30	56	2	28
Xie C[90]	9	5	0	5
Total	1371	500	55	340

RT-PCR, real-time polymerase chain reaction; TP, true positive; FP, false positive; FN, false negative; TN, true negative.

set are displayed in Table 6. In general, COVID-19 pneumonia can be divided into early, progressive, severe and dissipative stage according to the onset time and the course of disease. The patients in the early stage are more likely to present with pure GGO and halo sign (42). With the progression of the disease, GGO lesions gradually decreased, and the consolidation lesions first increased and then remained relatively stable for a certain period of time (6–13 days). The lesions are always absorbed and fibrosis increased after 14 days, and the lesion absorption may extend beyond 26 days (91). Wang et al. (101) evaluated the longitudinal changes and also found that GGO was the most common radiological finding following the onset of symptoms, while GGO mixed with irregular linear opacity peaked at 6–11 days after the onset. It is important to note that lesions' evolution on CT varied with disease severity. The lung lesions in patients with moderate stage peak on 13–15 days, while opacity volume in the severe/critical patients continue to increase after 15 days. Asymptomatic/mild patients have smaller extent of pulmonary abnormalities which almost resolve after 15 days (102).

Follow-up imaging was obtained in 15 studies (Table 7). Because of heterogeneity across follow-up intervals, inconsistent findings were reported. Lesions smaller or disappearing and/or consolidations converting to GGO indicated improvement. Some patients showed progressive disease with more GGO, enlarged and consolidated, and enlarged fibrous strips. In general, children had a better performance on CT during follow-up.

Discussion

This review provided an evaluation of pulmonary infiltration of COVID-19 on initial and follow-up chest CT from published literature. The abnormal initial CT findings comprise 92.61% (4961/5357) of the included patients. However, a recent study has shown that the sensitivity of chest CT to identify COVID-19 ranged from 44% to 97% depending on the sample size (103). When compared with RT-PCR results, CT findings have a sensitivity of 96.14% but a low specificity of 40.48% in diagnosing COVID-19, similar to the results of a meta-analysis (16). In the detection of COVID-19, CT is often used together with RT-PCR, which could mathematically guarantee optimal sensitivity of CT and retaining the high specificity of RT-PCR. It was an important part of managing the epidemic effectively and rapidly in China. Therefore, CT can be a valuable screen tool for identifying COVID-19.

This review summarized the main radiological findings of the literature. Imaging patterns of multiple peripheral GGO, mixed GGO with consolidation, or consolidation, distributed prominently in bilateral lungs and in the lower lung zones were considered highly for suspicious of COVID-19 pneumonia. These findings can be further confirmed by a positive real-time RT-PCR assay. Besides, other common features such as opacities with air bronchogram, vascular enlargement, bronchial wall thickening, "crazy-paving" pattern, reticulation, interlobular septal thickening, halo sign, reverse halo sign, bronchiectasis and pulmonary fibrosis have been reported. Interestingly, the halo sign and reverse halo sign were quite common in patients with COVID-19, which are more commonly seen on various fungal of infection (104). Nodules and intralobular septal thickening were uncommon. Pleural thickening was common findings in COVID-19, but other accompanying signs including pleural effusion, lymphadenopathy and pericardial effusion were uncommon. Additionally, pneumothorax was reported in a COVID-19 case (105), but it was unknown if it was a direct complication of the coronavirus infection. Nevertheless, there are still a subset of patients with confirmed COVID-19 showing normal findings on initial CT (10, 33–35, 39, 53, 54, 73–79), especially in early stage of COVID-19. Thus repeated CT scans might be required in such patients.

CT manifestations of COVID-19 can be diverse, depending on the immune status (age or disease severity) of the patient. Young patients and older adults with COVID-19 may share certain CT features (20, 26, 28), but older patients (>60 years) are likely to have more lung involvement, and subpleural line, pleural thickening and consolidation (20, 28). Younger patients

Table 6. Time course of lung changes on chest CT

Author [Ref]	Time course (days)						
Pan F[91]	0–4	5–8		9–13		≥14	
	GGO in subpleural lower lobes unilaterally or bilaterally	Bilateral multi-lobe distribution with diffuse GGO, crazy-paving pattern and consolidation		Lung involvement increased to the peak and more consolidation. Findings included diffuse GGO, crazy-paving pattern, consolidation, and residual parenchymal band		The consolidation was gradually absorbed. Extensive GGO could be observed as the demonstration of the consolidation absorption	
Wang JC[92]	2–5	6–9		10–13		≥14	
	The main performance is GGO	The lesions rapidly progressed with lung involvement and consolidation		The lesions distinctly resolved, more fibrosis		Fibrosis obviously increased	
Ding X[93]	0–4	5–9	10–14	15–21		22–28	>28
	The main performance is GGO	Air bronchogram	Crazy-paving pattern	Consolidation and air bronchogram, pleural effusion		In-ear opacities	GGO and bronchiectasis
Shi H[41]	Scans done before symptom onset	<7		7–14		14–21	
	GGO	Bilateral, diffuse, GGO dominated		GGO+consolidation. The highest mean number of involved segments		GGO+reticular patterns	
Xiang Y[94]	0–4	5–9		10–14		>14	
	GGO frequently in the subpleural	An increased and mixed density (crazy-paving pattern) with mild consolidation		An expanded range of consolidation and linear lesions		A gradual resolution of the consolidation with more linear lesions	
Shang Y[95]	<7	7–14			14–21		
		More lung involvement and fibrosis than the first week			More lung lobes involved and more fibrosis		
Hu S[96]	1–2		3–6		7–10	14	
	Segmental or subsegmental GGO		Consolidation pattern appeared and the GGOs appeared in more cases gradually			GGOs mimicking nodules	
Zhou S[97]	1–7		8~14			>14	
	GGO + reticular pattern, GGO +consolidation, and GGO were all common		GGO + consolidation and repairing CT signs (subpleural line, bronchus distortion, and fibrotic strips) increase			GGO + consolidation sharply decreased	
Jiang X[98]	1–3	4–6	7–9	10–12	13–15	16–18	≥19
	GGO or GGO with reticular interlobular septal thickening	Increased GGO, consolidation partial fusion, and reticular interlobular septal thickening	Half of the lesions had progressed and a small amount of lesions were absorbed	Some disease progression and some lesions were absorbed	Began to be absorbed	Had better absorption	Further absorbed, but slower than in the earlier stage
Han X[99]	<7		7–21			21–28	
	GGO + enlarged pulmonary vessels in peripheral bilateral lung		Marked increase of mean CT score			Decrease of mean CT score	

GGO, ground glass opacity; d, day.

tend to have more GGOs (20). COVID-19 can be divided into mild, moderate, severe and critical types according to its severity and the imaging manifestations of different stages can overlap (6). The patients in the moderate stage are more likely to present with pure GGO and halo sign (42), while some mild patients can present with negative imaging findings (6, 85). Pathological findings from two early stage patients with GGO exhibited exudative and proliferative phase acute lung injury such as edema, inflammatory infiltrate, type II pneumocyte hyperplasia, and organization (106). The severe and critical types of COVID-19 usually involve both lungs and multiple lobes, present with consolidation with crazy-paving sign, interlobular septal thickening, pleural thickening, architectural distortion, bronchiectasis dominantly (33, 42, 47, 51). Besides, intrathoracic lymph node enlargement, pleural effusions and pericardial effusion are more likely to be found in the severe-critical group (33, 42, 47), probably because there is diffuse alveolar damage with cellular fibromyxoid exudates, and pulmonary edema with hyaline membrane formation in such patients (107).

Children were initially thought to be not susceptible to COVID-19, but pediatric patients suffered from COVID-19 gradually appeared following the emerging of familial cluster and the rapid increase in the number of infections. CT imaging has a lower sensitivity to detect pulmonary abnormality in children compared to adult patients. The presence and distribution of CT imaging findings of children are similar to those of adult patients. The GGO is the most

Table 7. Follow-up CT findings of COVID-19

Author [Ref]	Sample size	Follow-up data available (n)	Follow-up interval (days)	Changes on CT
Pan Y[21]	63	54	3–14	54 progressed
Liu RR[22]	33	22	3–5	6 improved, 10 progressed, 6 unchanged
Wu J[23]	130	35	/	21 improved (13 with partially absorbed and newly formed lesions, 14 with fibrosis), 14 progressed
Guan C[30]	53	33	2–12	8 improved, 25 progressed, 9 with partially absorbed and newly formed lesions, 2 with new pleural effusion
Xu Xi[48]	90	52/90	1–6	10 unchanged, 4 absorbed, 38 progressed
Wang X[49]	40	15/40	Mean 3.27	4 improved and 11 progressed
Xu YH[51]	50	30/50	3–13	18 improved, 10 progressed, 2 remained normal
Hu R[56]	105	87	2–4	15 improved and 72 progressed
Zhang L[71]	34	19	3–5	1 unchanged, 18 progressed
Ma J[72]	22	6	6–12	1 with negative CT stayed normal, 5 with positive CT (2 improved, presenting decreased density and smaller size, 1 obvious progressed, 1 unchanged, 1 with newly formed GGO)
Chen J[73]	20	20	3–5	New pneumonia emerging in 3 patients with initial normal CT, 10 improved, 4 with new lesions, 3 unchanged
Song W[74]	16	/	4–7	Improved
Feng K[76]	15	15	3–5	6 with negative CT, 3 stayed normal and 3 with new nodular GGO; Of the 9 patients with positive CT, 2 improved and 7 unchanged
Li YJ[78]	15	7	5–11	5 absorbed completely, and 2 improved
Steinberger S[80]	30	11	Mean 2.9	7 with negative CT stayed normal, 4 with positive CT (3 unchanged, 3 with partially absorbed and newly formed lesions)

GGO, ground glass opacity.

common findings and halo sign is a common ancillary finding in children patients. A recent study found that consolidation with surrounding halo sign was common in pediatric patients, which was different from adults (75). Nonetheless, children with COVID-19 show significantly lower incidences of some ancillary findings than adults. Intralobular septal thickening, pulmonary fibrosis, and bronchiectasis are not seen in children patients. There is only one child patient with enlarged lymph nodes (74) and two with pleural effusion (73, 82) in this systematic review. In COVID-19 positive children with little or only upper airway symptoms, 35%–50% of the cases may have a normal CT, and the sensitivity of CT to detect abnormalities in such patients range from 50% to 74% (103). Another study by Wu et al. (108) showed that higher proportion of asymptomatic cases (7.6%) are present among children than adults (1%), hence, the combination of CT imaging features with clinical and laboratory findings could contribute to the early identification of COVID-19 pneumonia in children.

CT manifestations of COVID-19 pneumonia change over time depending on the stage and severity of lung infection. Follow-up CT findings during the treatment could be helpful for effectively evaluating the treatment response of patients with COVID-19 (109). Fifteen studies with follow-up CT exams were analyzed in this review (21–23, 48–51, 56, 71–74, 76, 78, 80). Increasing GGO, enlarged and consolidated, and enlarged fibrous strips on CT indicate disease progression, while the smaller size, absorption of lesions indicate improvement during follow up. Lung abnormalities on chest CT show greatest severity 7–10 days after the initial onset of symptoms. The lesions always absorb and fibrosis increase after 14 days when the patient's condition was controlled and improved, revealing evidence of chronic involvement of the lungs. Pulmonary fibrosis is more likely to occur in older patients with severe illness during treatment (110). For COVID-19 patients who are about to be discharged, GGO and fibrosis are the main CT features that further regressed at 2–13 days of follow-up (111). These characteristics with dynamic changes on CT may help to monitor disease progression and clinical treatment. Studies have shown that compared with elderly COVID-19 patients, children or young adults have a good prognosis (112). Children with COVID-19 have a better performance on follow-up CT, which agree with recent systematic review reported before (113). The development of post-inflammatory fibrosis following viral pneumonia and adult respiratory distress syndrome has been well described (114). Further investigations are required to evaluate long-term or permanent lung damage for individuals recovering from COVID-19.

Finally, there were some limitations to this review. First, we only included the English studies and publications of the Chinese Medical Association. The Chinese literature should be reviewed for a more comprehensive assessment of the imaging findings. Second, we had not reviewed the reported findings in pregnant women with COVID-19. But the study by Wu X et al. (115) revealed that radiological findings in pregnant wom-

en with COVID-19 were similar to those of non-pregnant women on the chest CT. With the publication of new literature, updates of this systematic review will be necessary.

In conclusion, chest CT imaging is an important component in the diagnosis, staging, disease progression and follow-up of individuals with COVID-19, as supported by substantial evidence.

Conflict of interest disclosure

The authors declared no conflicts of interest.

References

1. Huang C, Wang Y, Li X, et al. Clinical features of patients infected with 2019 novel coronavirus in Wuhan, China. Lancet 2020; 395:497–506. [Crossref]
2. World Health Organization. WHO Director-General's remarks at the media briefing on 2019-nCoV on 11 February 2020. Available at: https://www.who.int/dg/speeches/detail/who-director-general-s-remarks-at-the-media-briefing-on-2019-ncov-on-11-february-2020. Published February 11, 2020.
3. Jiang X, Rayner S, Luo MH. Does sars-cov-2 has a longer incubation period than sars and mers? J Med Virol 2020; 92:476–478. [Crossref]
4. Fu L, Wang B, Yuan T, et al. Clinical characteristics of coronavirus disease 2019 (COVID-19) in China: a systematic review and meta-analysis. J Infect 2020; 80:656–665. [Crossref]
5. Corman VM, Landt O, Kaiser M, et al. Detection of 2019 novel coronavirus (2019-nCoV) by real-time RT-PCR. Euro Surveill 2020; 25. [Crossref]
6. National Health Commission of the People's Republic of China. Diagnosis and Treatment Protocols of Covid-19 Infection (6th ed). General Office of the National Health Commission, Medical Letter. Accessed on 18 Feb 2020.
7. Ai T, Yang Z, Hou H, et al. Correlation of chest CT and RT-PCR testing in coronavirus disease 2019 (COVID-19) in China: a report of 1014 cases. Radiology 2020; 200642. [Crossref]
8. Yang Y, Yang M, Shen C, et al. Evaluating the accuracy of different respiratory specimens in the laboratory diagnosis and monitoring the viral shedding of 2019-nCoV infections. medRxiv 2020. [Crossref]
9. Ng M, Lee EYP, Yang J, et al. Imaging profile of the COVID-19 infection: Radiologic findings and literature review. Radiol Cardiothorac Imaging 2020; 2:e200034. [Crossref]
10. Bernheim A, Mei X, Huang M, et al. Chest CT findings in coronavirus disease-19 (COVID-19): relationship to duration of infection. Radiology 2020; 295:200463. [Crossref]
11. Xie X, Zhong Z, Zhao W, Zheng C, Wang F, Liu J. Chest CT for typical 2019-nCoV pneumonia: relationship to negative RT-PCR testing. Radiology 2020; 200343.
12. Salehi S, Abedi A, Balakrishnan S, Gholamrezanezhad A. Coronavirus disease 2019 (COVID-19): a systematic review of imaging findings in 919 patients. AJR Am J Roentgenol 2020; 215:87–93. [Crossref]
13. Adams HJA, Kwee TC, Yakar D, Hope MD, Kwee RM. Systematic review and meta-analysis on the value of chest CT in the diagnosis of coronavirus disease (COVID-19): Sol Scientiae, Illustra Nos. AJR Am J Roentgenol 2020; 1–9. [Crossref]
14. Zhu J, Zhong Z, Li H, et al. CT imaging features of 4121 patients with COVID-19: A meta-analysis. J Med Virol 2020; 92:891–902. [Crossref]
15. Bao C, Liu X, Zhang H, Li Y, Liu J. Coronavirus disease 2019 (COVID-19) CT findings: a systematic review and meta-analysis. J Am Coll Radiol 2020; 17:701–709. [Crossref]
16. Kim H, Hong H, Yoon SH. Diagnostic performance of CT and reverse transcriptase-polymerase chain reaction for coronavirus disease 2019: A meta-analysis. Radiology 2020; 201343. [Crossref]
17. Huang L, Han R, Yu P, Wang S, Xia L. A correlation study of CT and clinical features of different clinical types of 2019 novel coronavirus pneumonia. Chin J Radiol 2020; 54:E003.
18. Lu X, Gong W, Wang L, et al. Clinical features and high resolution CT imaging findings of preliminary diagnosis novel coronavirus pneumonia. Chin J Radiol 2020; 54:E006.
19. Liu H, Zhang D, Yang Y, et al. Analysis of early chest high resolution CT images of novel coronavirus pneumonia. Chin J Radiol 2020; 54:E007.
20. Song F, Shi N, Shan F, et al. Emerging 2019 novel coronavirus (2019-nCoV) pneumonia. Radiology 2020; 295:210–217. [Crossref]
21. Pan Y, Guan H, Zhou S, et al. Initial CT findings and temporal changes in patients with the novel coronavirus pneumonia (2019-nCoV): a study of 63 patients in Wuhan, China. Eur Radiol 2020; 30:3306–3309. [Crossref]
22. Liu RR, Zhu Y, Wu MY, et al. CT imaging analysis of 33 cases with the 2019 novel coronavirus infection. Zhonghua Yi Xue Za Zhi 2020; 100:1007–1011.
23. Wu J, Feng CL, Xian XY, et al. Novel coronavirus pneumonia (COVID-19) CT distribution and sign features. Zhonghua Jie He He Hu Xi Za Zhi 2020; 43: E030.
24. Long C, Xu H, Shen Q, et al. Diagnosis of the coronavirus disease (COVID-19): rRT-PCR or CT? Eur J Radiol 2020; 126:108961. [Crossref]
25. Zhou Z, Guo D, Li C, et al. Coronavirus disease 2019: initial chest CT findings. Eur Radiol 2020; 1–9. [Crossref]
26. Chen Z, Fan H, Cai J, et al. High-resolution computed tomography manifestations of COVID-19 infections in patients of different ages. Eur J Radiol 2020; 126:108972. [Crossref]
27. Zhou S, Wang Y, Zhu T, Xia L. CT Features of Coronavirus Disease 2019 (COVID-19) Pneumonia in 62 Patients in Wuhan, China. AJR Am J Roentgenol 2020; 214:1287–1294. [Crossref]
28. Zhu T, Wang Y, Zhou S, Zhang N, Xia L. A comparative study of chest computed tomography features in young and older adults with corona virus disease (COVID-19). J Thorac Imaging 2020; 35:W97–W101. [Crossref]
29. Fan N, Fan W, Li Z, Shi M, Liang Y. Imaging characteristics of initial chest computed tomography and clinical manifestations of patients with COVID-19 pneumonia. Jpn J Radiol 2020; 38:533–538. [Crossref]
30. Guan CS, Lv ZB, Yan S, et al. Imaging features of coronavirus disease 2019 (COVID-19): evaluation on thin-section CT. Acad Radiol 2020; 27:609–613. [Crossref]
31. Han R, Huang L, Jiang H, Dong J, Peng H, Zhang D. Early clinical and CT manifestations of coronavirus disease 2019 (COVID-19) pneumonia. AJR Am J Roentgenol 2020; 1–6. [Crossref]
32. Jie B, Liu X, Suo H, et al. Clinical and dynamic computed tomography features of 24 patients with coronavirus disease 2019. Can Assoc Radiol J 2020. [Crossref]
33. Li K, Wu J, Wu F, et al. The clinical and chest CT features associated with severe and critical COVID-19 pneumonia. Invest Radiol 2020; 55:327–331. [Crossref]
34. Li K, Fang Y, Li W, et al. CT image visual quantitative evaluation and clinical classification of coronavirus disease (COVID-19). Eur Radiol 2020; 1–10. [Crossref]
35. Li X, Zeng W, Li X, et al. CT imaging changes of corona virus disease 2019 (COVID-19): a multi-center study in Southwest China. J Transl Med 2020; 18:154. [Crossref]
36. Li Y, Xia L. Coronavirus disease 2019 (COVID-19): Role of chest CT in diagnosis and management. AJR Am J Roentgenol 2020; 214:1280–1286. [Crossref]
37. Liu KC, Xu P, Lv WF, et al. CT manifestations of coronavirus disease-2019: A retrospective analysis of 73 cases by disease severity. Eur J Radiol 2020; 126:108941. [Crossref]
38. Liu Z, Jin C, Wu CC, et al. Association between initial chest CT or clinical features and clinical course in patients with coronavirus disease 2019 pneumonia. Korean J Radiol 2020; 21:736–745. [Crossref]
39. Luo Z, Wang N, Liu P, et al. Association between chest CT features and clinical course of coronavirus disease 2019. Respir Med 2020; 168:105989. [Crossref]
40. Meng H, Xiong R, He R, et al. CT imaging and clinical course of asymptomatic cases with COVID-19 pneumonia at admission in Wuhan, China. J Infect 2020; 81:e33–e39. [Crossref]
41. Shi H, Han X, Jiang N, et al. Radiological findings from 81 patients with COVID-19 pneumonia in Wuhan, China: a descriptive study. Lancet Infect Dis 2020; 20: 425–434. [Crossref]
42. Wang J, Xu Z, Wang J, et al. CT characteristics of patients infected with 2019 novel coronavirus: association with clinical type. Clin Radiol 2020; 75:408–414. [Crossref]
43. Wang K, Kang S, Tian R, Zhang X, Zhang X, Wang Y. Imaging manifestations and diagnostic value of chest CT of coronavirus disease 2019 (COVID-19) in the Xiaogan area. Clin Radiol 2020; 75:341–347. [Crossref]
44. Wang M, Guo L, Chen Q, Xia G, Wang B. Typical radiological progression and clinical features of patients with coronavirus disease 2019. Aging (Albany NY) 2020; 12:7652–7659. [Crossref]
45. Wu J, Wu X, Zeng W, et al. Chest CT findings in patients with coronavirus disease 2019 and its relationship with clinical features. Invest Radiol 2020; 55:257–261. [Crossref]
46. Yang W, Cao Q, Qin L, et al. Clinical characteristics and imaging manifestations of the 2019 novel coronavirus disease (COVID-19):A multi-center study in Wenzhou city, Zhejiang, China. J Infect 2020; 80:388–393. [Crossref]
47. Zhang S, Li H, Huang S, You W, Sun H. High-resolution computed tomography features of 17 cases of coronavirus disease 2019 in Sichuan province, China. Eur Respir J 2020; 55:2000334. [Crossref]
48. Xu X, Yu C, Qu J, et al. Imaging and clinical features of patients with 2019 novel coronavirus SARS-CoV-2. Eur J Nucl Med Mol Imaging 2020; 47:1275–1280. [Crossref]

49. Wang X, Liu B, Yu Y, et al. Application value of chest multi-detector spiral CT in diagnosis and follow-up of corona virus disease 2019. Chinese J Med Imag Technol 2020; 36:400–404.
50. Caruso D, Zerunian M, Polici M, et al. Chest CT Features of COVID-19 in Rome, Italy. Radiology 2020; 296:E79–E85. [Crossref]
51. Xu YH, Dong JH, An WM, et al. Clinical and computed tomographic imaging features of novel coronavirus pneumonia caused by SARS-CoV-2. J Infect 2020; 80:394–400. [Crossref]
52. Xiong Y, Sun D, Liu Y, et al. Clinical and high-resolution CT features of the COVID-19 infection: comparison of the initial and follow-up changes. Invest Radiol 2020; 55:332–339. [Crossref]
53. Bai HX, Hsieh B, Xiong Z, et al. Performance of radiologists in differentiating COVID-19 from viral pneumonia on chest CT. Radiology 2020; 200823. [Crossref]
54. Yu CC, Qu J, Zhang LG, et al. High resolution CT findings and clinical features of novel coronavirus pneumonia in Guangzhou. Chinese J Radiol 2020; 54: E010.
55. Yang T, Yu XN, He XX, Zhou W, Fu YM, Feng QM. Early clinical manifestations and pulmonary imaging analysis of patients with novel coronavirus pneumonia. Chinese J Emergency Med 2020; 29:341–345.
56. Hu R, Huang N, Chen W, et al. Comparison of chest CT images between confirmed and suspected cases of COVID-19. Chinese J Radiol 2020; 54:E015.
57. Dai H, Zhang X, Xia J, et al. High-resolution chest CT features and clinical characteristics of patients infected with COVID-19 in Jiangsu, China. Int J Infect Dis 2020; 95:106–112. [Crossref]
58. Zhao W, Zhong Z, Xie X, Yu Q, Liu J. CT scans of patients with 2019 novel coronavirus (COVID-19) pneumonia. Theranostics 2020; 10:4606–4613. [Crossref]
59. Yu M, Liu Y, Xu D, Zhang R, Lan L, Xu H. Prediction of the development of pulmonary fibrosis using serial thin-section CT and clinical features in patients discharged after treatment for COVID-19 pneumonia. Korean J Radiol 2020; 21:746–755. [Crossref]
60. Haseli S, Khalili N, Bakhshayeshkaram M, Sanei Taheri M, Moharramzad Y. Lobar distribution of COVID-19 pneumonia based on chest computed tomography findings: a retrospective study. Arch Acad Emerg Med 2020; 8:e55.
61. Hu Q, Guan H, Sun Z, et al. Early CT features and temporal lung changes in COVID-19 pneumonia in Wuhan, China. Eur J Radiol 2020; 128:109017.[Crossref]
62. Liu M, Zeng W, Wen Y, Zheng Y, Lv F, Xiao K. COVID-19 pneumonia: CT findings of 122 patients and differentiation from influenza pneumonia. Eur Radiol 2020; 30:5463–5469. [Crossref]
63. Li X, Fang X, Bian Y, Lu J. Comparison of chest CT findings between COVID-19 pneumonia and other types of viral pneumonia: a two-center retrospective study. Eur Radiol 2020; 30:5470–5478. [Crossref]
64. Xiong Z, Xin C, Yan X, et al. Clinical characteristics and outcomes of 421 patients with COVID-19 treated in a mobile cabin hospital. Chest 2020; 158:939–946. [Crossref]
65. Liu J, Chen T, Yang H, et al. Clinical and radiological changes of hospitalised patients with COVID-19 pneumonia from disease onset to acute exacerbation: a multicentre paired cohort study. Eur Radiol 2020; 30:5702–5708. [Crossref]
66. Xie S, Lei Z, Chen X, et al. Chest CT-based differential diagnosis of 28 patients with suspected corona virus disease 2019 (COVID-19). Br J Radiol 2020; 93:20200243. [Crossref]
67. Fu F, Lou J, Xi D, et al. Chest computed tomography findings of coronavirus disease 2019 (COVID-19) pneumonia. Eur Radiol 2020; 30:5489–5498. [Crossref]
68. Wang H, Wei R, Rao G, Zhu J, Song B. Characteristic CT findings distinguishing 2019 novel coronavirus disease (COVID-19) from influenza pneumonia. Eur Radiol 2020; 30:4910–4917. [Crossref]
69. Yin Z, Kang Z, Yang D, Ding S, Luo H, Xiao E. A Comparison of Clinical and Chest CT Findings in Patients With Influenza A (H1N1) Virus Infection and Coronavirus Disease (COVID-19). AJR Am J Roentgenol 2020 May 26. [Epub Ahead of Print] [Crossref]
70. Nie W, Feng Z, Mao X, Rong P, Wang W, Liang Q. First CT characteristic appearance of patients with coronavirus disease 2019. Zhong Nan Da Xue Xue Bao Yi Xue Ban 2020; 45:262–268.
71. Zhang L, Kong X, Li X, et al. CT imaging features of 34 patients infected with COVID-19. Clin Imaging 2020; 68:226–231. [Crossref]
72. Ma J, Shao J, Wang Y, et al. High resolution CT features of novel coronavirus pneumonia in children. Chin J Radiol 2020; 54:E002.
73. Chen J, Wang XF, Zhang PF. Asymptomatic SARS-CoV-2 infection in children: a clinical analysis of 20 cases. Chin J Contemp Pediatr 2020; 1–5.
74. Song W, Li J, Zou N, Guan W, Pan J, Xu W. Clinical features of pediatric patients with coronavirus disease (COVID-19). J Clin Virol 2020; 127:104377. [Crossref]
75. Xia W, Shao J, Guo Y, Peng X, Li Z, Hu D. Clinical and CT features in pediatric patients with COVID-19 infection: Different points from adults. Pediatr Pulmonol 2020; 55:1169–1174. [Crossref]
76. Feng K, Yun Y, Wang X, et al. Analysis of CT features of 15 children with 2019 novel coronavirus infection. Zhonghua Er Ke Za Zhi 2020; 58:E007.
77. Zheng F, Liao C, Fan QH, et al. Clinical characteristics of children with coronavirus disease 2019 in Hubei, China. Curr Med Sci 2020; 40:275–280. [Crossref]
78. Li YJ, Ye YF, Xuan WL, Chen YJ, Wu BL, Chen ZH. Imaging features of the initial chest high resolution CT scan in juvenile patient with Coronavirus disease 2019. Chin J Gen Pract 2020; 19:E004.
79. Li B, Shen J, Li Liang, Yu CX. Radiographic and clinical features of children with coronavirus disease (COVID-19) pneumonia. Indian Pediatr 2020; 57:423–426. [Crossref]
80. Steinberger S, Lin B, Bernheim A, et al. CT features of coronavirus disease (COVID-19) in 30 pediatric patients. AJR Am J Roentgenol 2020 May 22; 1–9. [Epub Ahead of Print] [Crossref]
81. Wu HP, Li BF, Chen X, et al. Clinical features of coronavirus disease 2019 in children aged <18 years in Jiangxi, China: an analysis of 23 cases. Zhongguo Dang Dai Er Ke Za Zhi 2020; 22:419–424.
82. Ma H, Hu J, Tian J, et al. A single-center, retrospective study of COVID-19 features in children: a descriptive investigation. BMC Med 2020; 18:123. [Crossref]
83. Zhong Q, Li Z, Shen X, et al. CT imaging features of patients with different clinical types of coronavirus disease 2019 (COVID-19). Zhejiang Da Xue Xue Bao Yi Xue Ban 2020; 49: 0.
84. Guo F, Zhu L, Xu H, Qin L, Liang X, Deng X. Correlation between clinical classification of COVID-19 and imaging characteristics of MSCT volume scanning of the lungs. Nan Fang Yi Ke Da Xue Xue Bao 2020; 40:321–326.
85. Deng ZQ, Zhang XC, Li YR, et al. Value of chest CT screening in the early COVID-19 outbreak. Chin J Radiol 2020; 54.
86. He JL, Luo L, Luo ZD, et al. Diagnostic performance between CT and initial real-time RT-PCR for clinically suspected 2019 coronavirus disease (COVID-19) patients outside Wuhan, China. Respir Med 2020; 168:105980. [Crossref]
87. Wen Z, Chi Y, Zhang L, et al. Coronavirus disease 2019 initial detection on chest CT in a retrospective multicenter study of 103 Chinese Subjects. Radiol Cardiothorac Imaging 2020; 2. [Crossref]
88. Himoto Y, Sakata A, Kirita M, et al. Diagnostic performance of chest CT to differentiate COVID-19 pneumonia in non-high-epidemic area in Japan. Jpn J Radiol 2020; 38:400–406. [Crossref]
89. Zhu W, Xie K, Lu H, Xu L, Zhou S, Fang S. Initial clinical features of suspected coronavirus disease 2019 in two emergency departments outside of Hubei, China. J Med Virol 2020 Mar 13. [Epub Ahead of Print] [Crossref]
90. Xie C, Jiang L, Huang G, et al. Comparison of different samples for 2019 novel coronavirus detection by nucleic acid amplification tests. Int J Infect Dis 2020; 93:264–267. [Crossref]
91. Pan F, Ye T, Sun P, et al. Time course of lung changes at chest CT during recovery from coronavirus disease 2019 (COVID-19). Radiology 2020; 295:715–721.[Crossref]
92. Wang J, Liu J, Wang Y, et al. Dynamic changes of chest CT imaging in patients with corona virus disease-19 (COVID-19). Zhejiang Da Xue Xue Bao Yi Xue Ban 2020; 49:0. [Crossref]
93. Ding X, Xu J, Zhou J, Long Q. Chest CT findings of COVID-19 pneumonia by duration of symptoms. Eur J Radiol 2020; 127:109009. [Crossref]
94. Xiang Y, Yang Q, Sun H, Qin X, Li X, Zhang Q. Chest CT findings and their dynamic changes in patients with COVID-19. Nan Fang Yi Ke Da Xue Xue Bao 2020; 40:327–332.
95. Shang Y, Xu C, Jiang F, et al. Clinical characteristics and changes of chest CT features in 307 patients with common COVID-19 pneumonia infected SARS-CoV-2: A multicenter study in Jiangsu, China. Int J Infect Dis 2020; 96:157–162. [Crossref]
96. Hu S, Li Z, Chen X, Liang CH. Computed tomography manifestations in super early stage 2019 novel coronavirus pneumonia. Acta Radiol 2020 May 21; 284185120924806. [Epub Ahead of Print] [Crossref]

97. Zhou S, Zhu T, Wang Y, Xia L. Imaging features and evolution on CT in 100 COVID-19 pneumonia patients in Wuhan, China. Eur Radiol 2020; 1–9. [Crossref]
98. Jiang X, Yin Z, Wang T, et al. COVID-19 dynamic computed tomography (CT) performance and observation of some laboratory indicators. Med Sci Monit 2020; 26:e924403. [Crossref]
99. Han X, Cao Y, Jiang N, et al. Novel coronavirus pneumonia (COVID-19) progression course in 17 discharged patients: comparison of clinical and thin-section CT features during recovery. Clin Infect Dis 2020; 71:723–731. [Crossref]
100. Wang Y, Hou H, Wang W, Wang W. Combination of CT and RT-PCR in the screening or diagnosis of COVID-19. J Glob Health 2020; 10:010347. [Crossref]
101. Wang Y, Dong C, Hu Y, et al. Temporal changes of CT findings in 90 patients with COVID-19 pneumonia: a longitudinal study. Radiology 2020 Mar 19; 200843. [Epub Ahead of Print] [Crossref]
102. Wang YC, Luo H, Liu S, et al. Dynamic evolution of COVID-19 on chest computed tomography: experience from Jiangsu Province of China. Eur Radiol 2020; 1–10. [Crossref]
103. Merkus PJFM, Klein WM. The value of chest CT as a COVID-19 screening tool in children. Eur Respir J 2020; 55:2001241. [Crossref]
104. Marom EM, Kontoyiannis DP. Imaging studies for diagnosing invasive fungal pneumonia in immunocompromised patients. Curr Opin Infect Dis 2011; 24:309–314. [Crossref]
105. Chen N, Zhou M, Dong X, et al. Epidemiological and clinical characteristics of 99 cases of 2019 novel coronavirus pneumonia in Wuhan, China: a descriptive study. Lancet 2020; 395:507–513. [Crossref]
106. Tian S, Hu W, Niu L, Liu H, Xu H, Xiao SY. Pulmonary pathology of early-phase 2019 novel coronavirus (COVID-19) pneumonia in two patients with lung cancer. J Thorac Oncol 2020; 15:700–704. [Crossref]
107. Xu Z, Shi L, Wang Y, et al. Pathological findings of COVID-19 associated with acute respiratory distress syndrome. Lancet Respir Med 2020; 8:420–422. [Crossref]
108. Wu Z, McGoogan JM. Characteristics of and important lessons from the coronavirus disease 2019 (COVID-19) outbreak in China: summary of a report of 72 314 cases from the Chinese center for disease control and prevention. JAMA 2020; 323:1239–1242. [Crossref]
109. Wei Z, Zheng Z, Xie X, Yu Q, Liu J. CT scans of patients with 2019 novel coronavirus (COVID-19) pneumonia. Theranostics 2020; 10:4606–4613. [Crossref]
110. Lei P, Fan B, Mao J, Wei J, Wang P. The progression of computed tomographic (CT) images in patients with coronavirus disease (COVID-19) pneumonia. J Infect 2020; 80:e30–e31. [Crossref]
111. Du S, Gao S, Huang G, et al. Chest lesion CT radiological features and quantitative analysis in RT-PCR turned negative and clinical symptoms resolved COVID-19 patients. Quant Imaging Med Surg 2020; 10:1307–1317. [Crossref]
112. Chen ZM, Fu JF, Shu Q, et al. Diagnosis and treatment recommendations for pediatric respiratory infection caused by the 2019 novel coronavirus. World J Pediatr 2020; 16:240–246. [Crossref]
113. Ludvigsson JF. Systematic review of COVID-19 in children shows milder cases and a better prognosis than adults. Acta Paediatr 2020; 109:1088–1095. [Crossref]
114. Mineo G, Ciccarese F, Modolon C, et al. Post-ARDS pulmonary fibrosis in patients with H1N1 pneumonia: role of follow-up CT. Radiol Med 2012; 117:185–200. [Crossref]
115. Wu X, Sun R, Chen J, Xie Y, Zhang S, Wang X. Radiological findings and clinical characteristics of pregnant women with COVID-19 pneumonia. Int J Gynaecol Obstet 2020; 150:58–63. [Crossref]